

Magnetic Resonance Imaging Noise Filtering using Adaptive Polynomial-Fit Non-Local Means

Chean-Khim Toa, Kok-Swee Sim, Zheng-You Lim, Chee-Peng Lim

Abstract— Every image, whether it is a Magnetic Resonance (MR) image or a gray scale image, usually contains noise, which negatively affects image processing and analysis outcomes. For MR images, noise can be induced by environmental, equipment, and human factors. Rician noise obeys a Rician distribution. It degrades the quality of an image and makes it blurry. Rician noise is signal-dependent. Thus, it is a difficult task to separate signals from noise. In order to reduce Rician noise in MR images, noise-removing techniques are necessary to be applied before the image undergoes further processing. In this paper, a noise-removing technique is developed by cascading a new noise estimation method known as Nonlinear Spatial Mean Absolute Deviation (NSMAD) with a new noise filter known as Adaptive Polynomial-Fit Non-Local Means (Adaptive_PFNLM) filter. The NSMAD method is used to estimate the level of noise standard deviation in MR images. Then, the value of noise standard deviation is passed to the Adaptive_PFNLM filter to remove noise. The NSMAD method is compared with three existing estimation methods, namely Brummer's method, Maximum Likelihood (ML) method, and Local Mean method. The Adaptive_PFNLM filter is also compared with three existing filters, namely Non-Local Means (NLM) filter, Linear Minimum Mean Square Error (LMMSE) filter, and Polynomial-Fit Non-Local Means (PFNLM) filter. The comparison is evaluated by using the mean absolute error (MAE), signal-to-noise ratio (SNR), mean square error (MSE), peak signal-to-noise ratio (PSNR), structure similarity (SSIM) and quality index (Q). The results indicate that NSMAD and Adaptive_PFNLM perform better than the existing noise estimation methods and noise filters.

Index Terms— Adaptive, MRI, Noise Estimation, Noise Filter, Rician Noise

I. INTRODUCTION

NOISE usually degrades the quality of an image, whether it is a gray scale image or a Magnetic Resonance (MR) image. Noise in MR images can be caused by environmental, equipment, and operator performance [1], [2]. Rician noise is classified as signal-dependent noise. Rician noise can degrade

the processing and interpretation of Magnetic Resonance Imaging (MRI) data [3], [4]. It can negatively affect the analysis of an image. The Rician distribution is formed by two uncorrelated nonlinear Gaussian distribution variables, i.e. magnitudes of the real and imaginary images. This kind of MRI noise is no longer known as Gaussian noise [5].

According to the Rician distribution, the magnitude of MR image is generated by first obtaining the real and imaginary signal magnitude values. Then, zero-mean uncorrelated Gaussian noise [6] is added to both values in order to corrupt the signals [7]. Comparing with the real and imaginary signals, the magnitude is comparably easier to be used. It is able to prevent the effects of incident phase variations. These variations usually are caused by a non-central sampling window, system delay, and Radio Frequency (RF) angle in homogeneity [8]. The magnitude data are obtained by using nonlinear operation. The Gaussian probability density function (GPDF) is transformed into the Rician probability density function (RPDF) by using the nonlinear operation [9].

Before filtering the images, noise estimation must first be implemented to estimate the amount of Rician noise. Three existing noise estimation methods, namely Brummer's method, Maximum Likelihood (ML) method, and Local Mean method are discussed in this paper. These estimation methods are used for comparison with the Nonlinear Spatial Mean Absolute Deviation (NSMAD) method.

In order to reduce Rician noise, a noise filter is implemented [10]. Three existing noise filters known as Non-Local Means (NLM), Linear Minimum Mean Square Error (LMMSE), and Polynomial-Fit Non-Local Means (PFNLM) are discussed in this paper. The proposed filter is based on concatenation of PFNLM and a Two-Dimensional (2-D) Adaptive Noise-Removal filter, which is denoted as the Adaptive_PFNLM filter. The three existing filters are compared with the proposed method. In this paper, MR images of various noise levels are applied to evaluate the noise estimation accuracy and performance of the proposed noise filter.

This paper is arranged as follows. A few prevailing noise estimation methods and noise filters are discussed in the next section. The details of proposed method are elaborated in Section III. In Section IV, the results and discussion pertaining to comparison between the proposed and existing methods are presented. In Section V, a summary of the outcome of the proposed method is described.

Manuscript received March 05, 2018; revised January 14, 2019. This work was supported in part by the Multimedia University Malaysia.

C. K. Toa, K. S. Sim and Z. Y. Lim are with the Faculty of Engineering and Technology, Multimedia University, Jalan Ayer Keroh Lama, 75450 Melaka, Malaysia (email: toacheankhim@yahoo.com; kssim@mmu.edu.my; zhengyou_93@live.com)

C. P. Lim is with the Institute for Intelligent Systems Research and Innovation, Geelong Waurn Ponds Campus, Deakin University, Geelong VIC 3220, Australia (email: chee.lim@deakin.edu.au)

II. REVIEW OF EXISTING NOISE ESTIMATION METHODS AND NOISE FILTERS

Noise estimation is an important step to execute before filtering out noise. The methods for noise estimation can be divided into two categories: multiple images and single image. The multiple images method used to estimate the noise level is based on acquiring two identical images under exact imaging conditions with a similar sampling area [11]. However, it is impossible to acquire similar measurements for both images. In addition, experiments with limited imaging time and functional studies are sometimes discouraged to repeat for the second time to derive image noise [12]. With this limitation, researchers prefer to use the single image method [13]. Based on the single image method, the noise standard deviation is estimated from a large and non-uniform region or a uniform region of a single magnitude image [11]. This method does not encounter the alignment problem because it only estimates noise from an image, while the multiple images method estimates noise based on two identical images. Various single image methods such as Least square estimation, Maximum Likelihood (ML), and Local Mean methods have been developed [7], [11]. Both ML and Local Mean methods estimate noise based on the histogram of background image, which is a Rayleigh distribution.

Denosing is a fundamental process to remove Rician noise from a corrupted image while retaining important information. There are several filtering techniques to remove Rician noise. The Wavelet-Domain filter is able to adjust various signal and noise variations [14]. The drawback is that the filter can accidentally eliminate the entire signal that has a similar size of structure as that of noise. The Non-Local Means (NLM) filter is based on a non-local algorithm that averages all the pixels in an image [15]. However, its major shortcoming is the heavy computation load that requires a long processing time [16]. To reduce the processing time, the Polynomial-Fit Non-Local Means (PFNLM) filter is proposed. This filter can reduce the computational load faced by NLM through examining salient feature related to the pixels [16]. The Linear Minimum Mean Square Error (LMMSE) estimator, which is a spatial filter, eliminates noise at the edges and fine details in MR images [7]. The Two-Dimensional (2-D) Adaptive Noise-Removal filter is commonly used to tackle various types of noise, such as Gaussian noise, salt and pepper noise, and Rician noise that exists in images [17], [18].

A. Background of Rician and Rayleigh distributions

Noise that follows a Rician distribution is formed by calculating the magnitude through a combination of both real and imaginary images corrupted by Gaussian noise. Instead of using both real and imaginary images, a magnitude image is preferred [19]. This is because a magnitude image is able to eliminate the effects of the incident phase variation. The magnitude image equation is determined by calculating the magnitude from both real and imaginary images [5], as shown in (1).

$$M = \sqrt{(A + n_1)^2 + n_2^2}, \quad (1)$$

where A is the signal level, n_1 and n_2 are both zero-mean uncorrelated Gaussian noise, and M is the magnitude data.

The probability density function (PDF) of an MRI image that follows the Rician distribution is shown in (2) [20], [21]

$$p_M(M|A, \sigma_N) = \frac{M}{\sigma_N^2} e^{-\frac{M^2+A^2}{2\sigma_N^2}} I_0\left(\frac{AM}{\sigma_N^2}\right) u(M), \quad (2)$$

where I_0 is the modified zeroth order Bessel function of the first kind, $u(M)$ is the Heaviside step function that indicates the PDF expression of M , which is a positive value, and σ_N^2 is the variance of Gaussian noise in the real and imaginary signals.

The Rayleigh distribution only appears in the background regions where the signal level (A) and signal-to-noise ratio (SNR) are equal to zero. Therefore, the PDF of Rician distribution can be transformed to the PDF of Rayleigh distribution [7] as shown in (3)

$$p_M(M|\sigma_N) = \frac{M}{\sigma_N^2} e^{-\frac{M^2}{2\sigma_N^2}} u(M), \quad (3)$$

B. Existing MRI noise estimation methods

1) Brummer's Method

Brummer's method [22] is used to estimate the noise standard deviation from single MRI images. This method uses least squares estimation where the Rayleigh distribution is implemented as a partial histogram.

$$\hat{K}, \hat{\sigma}_{Br} = \arg \max \sum_{f=0}^{f_c} (h(f) - K \frac{f}{\sigma^2} e^{-\frac{f^2}{2\sigma^2}})^2, \quad (4)$$

where $\hat{\sigma}_{Br}$ is the estimated noise level, K is the noise amplitude, f is the noise frequency, f_c is the cutoff frequency, $h(\cdot)$ is the histogram function, and σ is the width of Rayleigh distribution implemented as a histogram. The cutoff frequency is shown in (5)

$$f_c = 2\sigma_{Br,0}, \quad (5)$$

where $\sigma_{Br,0}$ is an initial estimate of the noise level. This method tends to overestimate the noise standard deviation value.

2) Maximum Likelihood (ML) method

The principle of the ML method [11] in estimating the noise variance is based on the background of an image histogram. The joint PDF of histogram data [5] is as follows

$$p(\{n_i\}|\sigma, \{l_i\}) = \frac{N!}{\prod_{i=1}^K n_i!} \prod_{i=1}^K p_i^{n_i}(\sigma), \quad (6)$$

where $p(\cdot)$ is a probability function, n_i is the count number in the range $[l_{i-1}, l_i]$, K is the number of data samples, σ is the standard deviation, $l_i, i = \{0, \dots, K\}$ represent the histogram bins boundaries, N_k is the total number of observations within the partial histogram, and $p_i^{n_i}$ is the observation probability within the range $[l_{i-1}, l_i]$. The joint PDF of histogram is known as the likelihood function and its standard deviation (σ) is considered as a variable. The probability of the Rayleigh distribution is shown in (7)

$$p_i^{n_i}(\sigma) = \frac{(e^{-\frac{l_{i-1}^2}{2\sigma^2}} - e^{-\frac{l_i^2}{2\sigma^2}})}{(e^{-\frac{l_0^2}{2\sigma^2}} - e^{-\frac{l_K^2}{2\sigma^2}})}, \quad (7)$$

The ML estimator is then developed by minimizing $\ln(\cdot)$ with respect to the standard deviation (σ).

$$\hat{\sigma}_{ML,K} = \arg \min [N_K \ln \left(e^{-\frac{l_0^2}{2\sigma^2}} - e^{-\frac{l_K^2}{2\sigma^2}} \right) - \sum_{i=1}^K n_i \ln \left(e^{-\frac{l_{i-1}^2}{2\sigma^2}} - e^{-\frac{l_i^2}{2\sigma^2}} \right)], \quad (8)$$

where $\hat{\sigma}_{ML,K}$ is the estimated standard deviation. The noise standard deviation estimated by the ML method is approximately the same as that of the previous method. In addition, the ML method tends to overestimate the actual standard deviation.

3) Local Mean Method

The Local Mean method [7] estimates noise in images with the assumption that it follows the Rayleigh distribution in the background of an image. For noisy images, the noise standard deviation ($\hat{\sigma}_n$) can be estimated by using (9)

$$\hat{\sigma}_n = \sqrt{\frac{2}{\pi}} \text{mode}(\hat{\mu}_{1ij}), \quad (9)$$

where $\hat{\sigma}_n$ is the estimated standard deviation, $\hat{\mu}_{1ij}$ is the mean function, and $\text{mode}(\hat{\mu}_{1ij})$ is the mode of mean distribution as shown in (10), (11)

$$\hat{\mu}_{1ij} = \frac{1}{N} \sum_{i=1}^N R_i(\sigma^2), \quad (10)$$

$$\text{mode}(\hat{\mu}_{1ij}) = \sigma_n \sqrt{\frac{2(2N-1)N}{e}}, \quad (11)$$

where e is constant of 2.71854144, N is number of data samples in an image, $R_i(\sigma^2), i = \{1, \dots, N\}$ is the set of independent and identically distributed (IID) random variables. Noise estimation using the Local Mean method has better accuracy than those of the previous two methods. Furthermore, the Local Mean method is able to minimize the issue of overestimation of noise, which is encountered by the

previous two methods. Nevertheless, this method is unable to estimate noise in images with low SNR in the background.

C. Existing methods for noise filtering in MRI

1) Noise filtering based on Non-Local Means (NLM) Filter

The Non-Local Means (NLM) filter [15] is based on a non-local method that averaging the entire pixels in an MRI image. The filtered output $\langle \hat{u}(x_i) \rangle$ at the x_i position is computed as the average of entire pixels in the image,

$$\hat{u}(x_i) = \sum_{x_j \in \Omega_i} \omega(x_i, x_j) u(x_j), \quad (12)$$

where Ω_i is an entire image search window centred at the pixel x_i and $\omega(x_i, x_j)$ is the weight that depends on the similarity between pixels x_i and x_j as

$$\omega(x_i, x_j) = \frac{1}{Z} e^{-\frac{\|u(N_i) - u(N_j)\|_2^2}{h^2}}, \quad (13)$$

where Z is a normalization constant as shown in (14)

$$Z = \sum_j e^{-\frac{\|u(N_i) - u(N_j)\|_2^2}{h^2}}, \quad (14)$$

where N_i and N_j are patches centred at x_i and x_j . Note that $u(N_i)$ indicates an $N \times 1$ vector covering all the values of $u(x_j)$ at pixels $x_j \in N_i$. The NLM filter not only compares grey level values of single point, but also the geometrical configurations of the entire neighbourhood. This enables a robust comparison when the grey level values are noisy. However, the drawback of this filter is its complexity and long computation load due to calculating the distance between the patches.

$$\hat{A}_{ij}^2 = \langle M_{ij}^2 \rangle - 2\sigma_n^2 + K_{ij}(M_{ij}^2 - \langle M_{ij}^2 \rangle), \quad (15)$$

2) Noise filtering based on the Linear Minimum Mean Square Error (LMMSE) filter

The performance of the Linear Minimum Mean Square Error (LMMSE) filter [7] is related to the accuracy of noise estimation. If a suitable estimator is chosen, the filter shows a good performance in noise filtering. Based on the Rician distribution of a 2-D signal, the unknown intensity (\hat{A}_{ij}^2) in pixels i and j is formulated as (16)

$$\hat{A}_{ij}^2 = E\{A_{ij}^2\} + \frac{C_{A_{ij}^2 M_{ij}^2}}{C_{M_{ij}^2 M_{ij}^2}} (M_{ij}^2 - E\{M_{ij}^2\}), \quad (16)$$

$$C_{A_{ij}^2 M_{ij}^2} = E\{A_{ij}^2\} + 2E\{A_{ij}^2\}\sigma_n^2 - E\{A_{ij}^2\}E\{M_{ij}^2\}, \quad (17)$$

$$C_{M_{ij}^2 M_{ij}^2} = E\{M_{ij}^4\} - E\{M_{ij}^2\}^2, \quad (18)$$

where M_{ij}^2 is the observation vector, $C_{A_{ij}^2 M_{ij}^2}$ is the cross-covariance vector, and $C_{M_{ij}^2 M_{ij}^2}$ is the covariance matrix. By using the relationship from the magnitude signal,

$$E\{M_{ij}^2\} = E\{A_{ij}^2\} + 2\sigma_n^2, \quad (19)$$

$$E\{M_{ij}^4\} = E\{A_{ij}^4\} + 8\sigma_n^2 E\{A_{ij}^2\} + 8\sigma_n^4, \quad (20)$$

and the LMMSE filter can be written as

$$K_{ij} = 1 - \frac{4\sigma_n^2(\langle M_{ij}^2 \rangle - \sigma_n^2)}{\langle M_{ij}^4 \rangle - \langle M_{ij}^2 \rangle^2}, \quad (21)$$

$$\widehat{A}_{ij}^2 = \langle M_{ij}^2 \rangle - 2\sigma_n^2 + K_{ij}(M_{ij}^2 - \langle M_{ij}^2 \rangle), \quad (22)$$

3) Noise filtering based on the Polynomial-Fit Non-Local Means (PFNLM) filter

The Polynomial-Fit Non-Local Means (PFNLM) filter [16] is proposed to reduce the computational load faced by the NL-means method. The filter is applied to examine the important features related to the pixels. In order to extract these features, the least square estimate is used as shown in (23)

$$u \simeq X \cdot c, \quad (23)$$

where c is a vector equal to

$$c = \dots [c_0, c_{st}]^T, \quad (24)$$

X is a Least Square matrix which contains

$$X = \begin{bmatrix} 1 & s_1 & t_1 & \frac{1}{2}s_1^2 & \frac{1}{2}t_1^2 & s_1 t_1 \\ 1 & s_2 & t_2 & \frac{1}{2}s_2^2 & \frac{1}{2}t_2^2 & s_2 t_2 \\ \vdots & \vdots & \vdots & \vdots & \vdots & \vdots \\ 1 & s_N & t_N & \frac{1}{2}s_N^2 & \frac{1}{2}t_N^2 & s_N t_N \end{bmatrix}, \quad (25)$$

and vector u is

$$u = [u(s_1, t_1), \dots, u(s_N, t_N)]^T, \quad (26)$$

Vector u is used to arrange the number of pixels (N) contained in the patch. The aim of this filter is to compute the expected value of patch distance $\langle E\{\tilde{d}(x_i, x_j)\} \rangle$.

$$E\{\tilde{d}(x_i, x_j)\} = \frac{1}{N} E\{(c_i, c_j)^T X^T X (c_i - c_j)\} = \frac{1}{N} \text{tr}\{E\{X d d^T X^T\}\}, \quad (27)$$

where c_i and c_j are two coefficients, and $\tilde{d}(x_i, x_j)$ is a patch distance given by (28)

$$\tilde{d}(x_i, x_j) = \frac{1}{N} (c_i - c_j)^T X^T X (c_i - c_j), \quad (28)$$

By substituting $c = (X^T X)^{-1} X^T u$ into (27), the expected value of patch distance can be further simplified to

$$E\{\tilde{d}(x_i, x_j)\} = \frac{K}{N} \cdot E[d(x_i, x_j)], \quad (29)$$

and has an effective value of h_{eff}^2

$$h_{eff}^2 = \frac{\eta}{N} h^2, \quad (30)$$

$$h_{eff}^2 = \frac{\eta}{N} h^2, \quad (31)$$

The PFNLM filter is able to decrease the computational load faced by the NLM filter by checking only a subset of salient features associated with the pixels. Comparing both NLM with PFNLM filters in term of improvements for denoising of MR image, the PFNLM filter is nearly twice faster than the NLM filter. However, the PFNLM filter is unable to perform well when a very high SNR is considered, in which case over blurring in an image appears, therefore affecting the capability of removing noise in the image.

4) Noise filtering based on 2-D adaptive noise-removal filtering

The 2-D adaptive noise-removal filtering [17] is able to give an optimal way to gradually reduce the noisy components, and provide a better reconstruction of the original signal. This filter estimates the local mean and variance around each pixel, as shown in (32), (33)

$$\mu = \frac{1}{MN} \sum_{x_1, x_2 \in \eta} a^2(x_1, x_2), \quad (32)$$

$$\sigma^2 = \frac{1}{MN} \sum_{x_1, x_2 \in \eta} a^2(x_1, x_2) - \mu^2, \quad (33)$$

where μ is local mean around each pixel, σ^2 is local variance, and η is the m-by-n neighbourhood of each pixel. By using these estimates, it creates a pixel-wise Wiener filter

$$b(x_1, x_2) = \mu + \frac{\sigma^2 - v^2}{\sigma^2} (a(x_1, x_2) - \mu), \quad (34)$$

where v^2 is the noise variance.

III. THE PROPOSED NOISE FILTERING METHOD

In this section, a noise filter based on concatenation of the Polynomial-Fit Non-Local Means (PFNLM) filter and 2-D Adaptive Noise-Removal filter is proposed. Before implementing the noise filter, the standard deviation of noise is calculated by using the Nonlinear Spatial Mean Absolute Deviation (NSMAD) method.

Fig. 1 shows the procedures involved in estimating the standard deviation of noise from a single image. A column-wise neighbourhood operation from the non-linear spatial filtering [23] is used to remove outliers from the input image. After that, an output image is obtained, which is able to approximate the original structure and, at the same time, retain the detailed information of the important structure. The output image and noisy input image are used to detach Rician noise from the image. This can be accomplished by finding the differences between the output and input images. To find the amount of Rician noise in the image, the argument of maxima is calculated. This provides a robust statistical estimation of the standard deviation of noise.

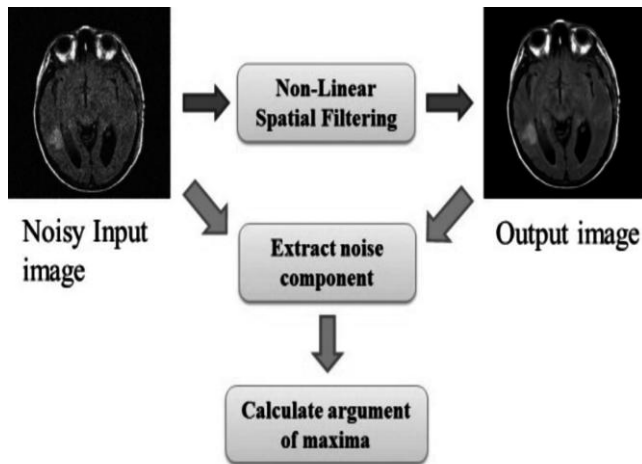


Fig. 1. The Single image estimation approach

Referring to nonlinear spatial filtering, a column process with a sliding neighbourhood operation based on the image pixels is shown in Fig. 2. The sliding neighbourhood operation involves the following steps:

1. Select a pixel from the noisy input image.
2. Determine the pixel's neighbourhood using an odd size n -by- n neighbourhood mask.
3. Reshape each sliding block of the pixel's neighbourhood into a column of a temporary matrix.
4. Apply the mean absolute deviation (MAD) function to the pixel values in the column. This function returns a scalar.
5. Repeat steps 1 to 4 for all pixels in the noisy input image.
6. Re-arrange all pixels to form the output image, which has the same size as that of the input image.

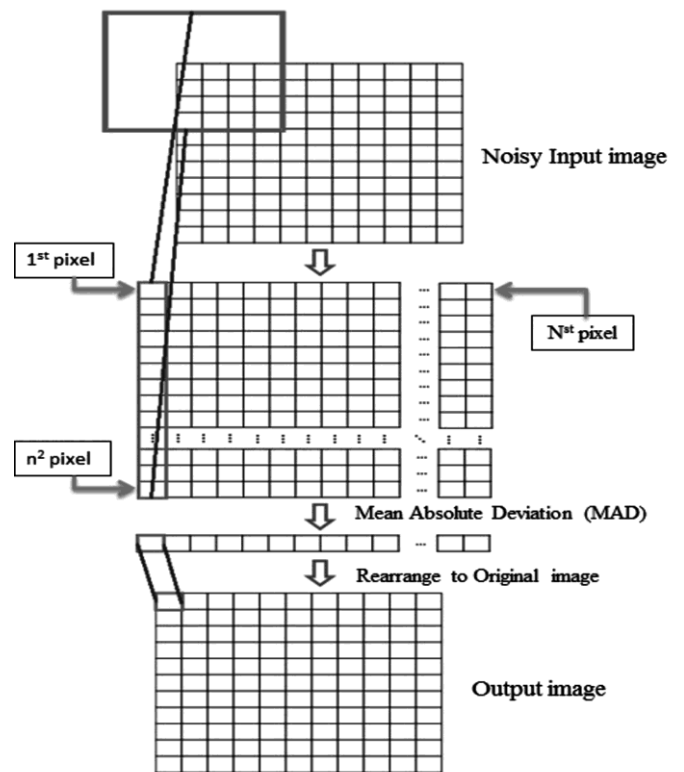


Fig. 2. Columnwise neighbourhood method

The formulation starts with the nonlinear spatial domain equation [24], [25]. In this equation, the mask, $T(s, t)$.

$$T(s, t) = \begin{bmatrix} T(-1, -1) & T(-1, 0) & \dots & T(-1, n) \\ T(0, -1) & T(0, 0) & \dots & T(0, n) \\ \vdots & \vdots & \ddots & \vdots \\ T(n, -1) & T(n, 0) & \dots & T(n, n) \end{bmatrix}, \quad (35)$$

and input data, $M_j(x + s, y + t)$.

$$M_j(x + s, y + t) = \begin{bmatrix} M_j(x - 1, y - 1) & M_j(x - 1, y) & \dots & M_j(x - 1, y + n) \\ M_j(x, y - 1) & M_j(x, y) & \dots & M_j(x, y + n) \\ \vdots & \vdots & \ddots & \vdots \\ M_j(x + n, y - 1) & M_j(x + n, y) & \dots & M_j(x + n, y + n) \end{bmatrix}, \quad (36)$$

are multiplied together to form output data, $G_j(x, y)$ as shown in (37)

$$G_j(x, y) = \sum_{s=-1}^n \sum_{t=-1}^n T(s, t) M_j(x + s, y + t), \quad j = \{1, \dots, N\}, \quad (37)$$

where N is the number of data of an input image, (s, t) is the mask coordinate, (x, y) is the coordinate of input image, $G_j(x, y)$ is the output image, $M_j(x + s, y + t)$ is the input image, and $T(s, t)$ is the odd size neighbourhood mask of n -by- n , which operates on $M_j(x + s, y + t)$ to determine the neighbourhood at coordinate (x, y) .

In MRI, the image background follows the Rayleigh distribution, $R_j(\sigma^2), j = \{1, \dots, N\}$ is shown in (38)

$$R_j(\sigma^2) = \frac{G_j}{\sigma} e^{\left(\frac{-G_j^2}{2\sigma^2}\right)}, j = \{1, \dots, N\}, \quad (38)$$

The pixels of the input image obey the Rayleigh distribution. The value of the Mean Absolute Deviation (MAD) [26] can be calculated using the data from a Rayleigh distribution as shown in (39), (40)

$$\mu_j = \frac{1}{N} \sum_{i=1}^{n^2} R_j(\sigma^2), \quad (39)$$

$$\text{MAD}_j = \frac{1}{N} \sum_{i=1}^{n^2} |R_j(\sigma^2) - \mu_j|, \quad (40)$$

where MAD_j is the of Mean Absolute Deviation for each pixel, μ_j is the average value, and N is the number of pixels in an odd side n -by- n neighbourhood mask. After that, each pixel of MAD_j is re-arranged to become the output image.

After obtaining the output image, which approximates the original image, the noise component can be separated from the noisy input image. Equation (41) shows the formulation to extract the noise component of each pixel from the noisy input image and output image.

$$x = (\text{Noisy Input image} - \text{Output image})^2, \quad (41)$$

where x is the noise component, the noisy input image is the one corrupted by Rician noise and the output image is similar to the original image. The pixel of the output image is subtracted from the noisy input image, and the square root with respect to the noise component is computed.

In single image, noise is achieved from a uniform and large noisy region where the distribution of an MR image follows the Rayleigh distribution [27]. According to the nonlinear spatial with the MAD function, the noise estimator ($\hat{\sigma}_E$) is formulated by multiplying the constant (C) with arguments of the maxima of a function (p_{MAD}) defined on a set domain (D). This estimator is shown in (42).

$$\hat{\sigma}_E = (C) \operatorname{argmax}_{M_j \in D} \{p_{MAD}(x)\}, \quad (42)$$

$$p_{MAD}(x) = \frac{x^{2N-1} e^{\frac{-x^2}{2bN}}}{2^{N-1} N^N b^N (N-1)!}, \quad (43)$$

$$b = \frac{\sigma^2}{N} \left(\frac{2N}{e}\right), \quad (44)$$

where N is the number of data of an image, $p_{MAD}(x)$ is the probability distribution of the noise component; M_j is the domain (D) input, which is able to achieve the highest function value.

Constant (C) is calculated based on a range of noise

standard deviations as shown in (45)

$$C = \frac{\sum_{\sigma=0.01}^{0.1} \frac{\sigma}{\operatorname{mode}(\mu)}}{10}, \quad (45)$$

The mode of a Rayleigh distribution ($\operatorname{mode}(\mu) = (\alpha - 1)\beta$) follows a Gamma distribution with parameters $\alpha = N$, $\beta = \frac{\sqrt{2}\sigma_{max}}{N}$, and $\sigma_{max} = m_{max}$. As such, the mode of the MAD moment is shown in (46)

$$\operatorname{mode}(\mu) = (N - 1) \frac{\sqrt{2}m_{max}}{N}, \quad (46)$$

where N is the number of data of an image, m_{max} is the maximum value of the histogram. The Nonlinear Spatial Mean Absolute Deviation (NSMAD) equation is

$$\hat{\sigma}_E = (C) \operatorname{argmax}_{\text{MAD}_j \in D} \left\{ \frac{x_{\text{MAD}_j}^{2N-1} e^{\frac{-x_{\text{MAD}_j}^2}{2bN}}}{2^{N-1} N^N b^N (N-1)!} \right\}, \quad (47)$$

Originally, the 2-D Adaptive Noise-Removal filter is a type of linear filter capable of removing noise in an MR image by involving the use of i and j kernel dimensions. By implementing the expected value of patch distance ($E\{\tilde{d}(x_1, x_2)\}$) of PFNLM into the formulation of local mean (51) and local variance (52), the proposed method can be developed as

$$c_i = (X^T X)^{-1} X^T u_i, \quad (48)$$

$$c_j = (X^T X)^{-1} X^T u_j, \quad (49)$$

$$E\{\tilde{d}(x_1, x_2)\} = \frac{1}{N} E \left\{ (c_i, c_j)^T X^T X (c_i - c_j) \right\}, \quad (50)$$

$$\mu = \frac{1}{MN} \sum_{x_1, x_2 \in \eta} E\{\tilde{d}(x_1, x_2)\}, \quad (51)$$

$$\sigma^2 = \frac{1}{MN} \sum_{x_1, x_2 \in \eta} E^2\{\tilde{d}(x_1, x_2)\} - \mu^2, \quad (52)$$

where c_i and c_j are two coefficients, σ^2 is local variance, μ is the local mean of each pixel, and η is the m -by- n neighbourhood of each pixel. Instead of just using i and j kernel dimensions, the standard deviation of noise based on the NSMAD method is introduced into the filter

$$\text{Adaptive_PFNLM}(x_1, x_2) = \mu + \frac{\sigma^2 - \hat{\sigma}_E^2}{\sigma^2} [E\{\tilde{d}(x_1, x_2)\}], \quad (53)$$

where $\hat{\sigma}_E$ is the standard deviation of noise for the NSMAD method.

Algorithm 1: Adaptive Polynomial-Fit Non-Local Means

- 1: Read the input images, M_j
- 2: Generate the pixel neighbourhood, G_j
- 3: Calculate the Rayleigh distribution, $R_j(\sigma^2)$ using G_j
- 4: Calculate the Mean Absolute Deviation, MAD_j
- 5: Generate the noisy component, $x = (\text{Noisy Input image} - \text{Output image})^2$
- 6: Formulate the noise estimator $\langle \hat{\sigma}_E \rangle$
- 7: Calculate the local variance σ^2 and local mean μ
- 8: Apply the formula of $\mu + \frac{\sigma^2 - \hat{\sigma}_E^2}{\sigma^2} [E(\tilde{d}(x_1, x_2))]$ for noise filtering.
- 9: End

The steps involved in the proposed method are shown in Fig. 3.

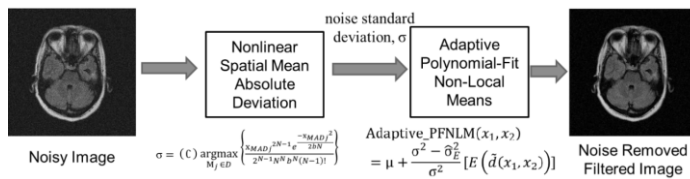


Fig. 3. Steps of the proposed method

IV. RESULTS AND DISCUSSION

In this section, the NSMAD method is compared with three existing estimation methods namely Brummer's method, Maximum Likelihood (ML) method, and Local Mean method. For noise filtering, the Adaptive_PFNLM filter is compared with three existing filters, i.e. Non-Local Means (NLM) filter, Linear Minimum Mean Square Error (LMMSE) filter, and Polynomial-Fit Non-Local Means (PFNLM) filter. The MATLAB software is used as the platform to develop all noise estimation methods and noise filters.

To measure the level of accuracy of the proposed noise estimation method and noise filter, a number of quality metrics such as signal-to-noise ratio (SNR), mean square error (MSE), peak signal-to-noise ratio (PSNR), structure similarity (SSIM) and quality index (Q) have been used.

The estimated noise standard deviation, $\hat{\sigma}_E$ calculated by the existing and proposed methods are used as the input data for the estimated noisy image, $M_E(x, y)$.

$$M_E(x, y) = \sqrt{[A(x, y)]^2 + 2\hat{\sigma}_E^2}, \quad (54)$$

where $A(x, y)$ is the original image and $\hat{\sigma}_E$ is the estimated noise standard deviation using the existing and proposed methods.

For the actual noisy image, $M_N(x, y)$, the equation is

$$M_N(x, y) = \sqrt{[A(x, y)]^2 + 2\sigma_n^2}, \quad (55)$$

where $A(x, y)$ is the original image and σ_n is the actual standard deviation.

After that, the actual and estimated noisy image equations are substituted into the SNR equation as shown, as shown in (56)

$$SNR \text{ (dB)} = 10 \log_{10} \left[\frac{\sum_0^{n_x-1} \sum_0^{n_y-1} [r(x, y)]^2}{\sum_0^{n_x-1} \sum_0^{n_y-1} [r(x, y) - M(x, y)]^2} \right], \quad (56)$$

where $[n_x, n_y]$ is the size of images, $M(x, y)$ is noisy image with an unknown standard deviation $\langle \sigma \rangle$ of noise, and $r(x, y)$ is the reference image (noise-free image). The size $[n_x, n_y]$ of two images must be same. This SNR equation can be divided into actual SNR value $\langle SNR_N \rangle$ of σ_n and estimated SNR value $\langle SNR_E \rangle$ of $\hat{\sigma}_E$.

Moreover, accuracy of the estimated SNR value can be computed by referring to the absolute error between SNR_N and SNR_E as shown in (57)

$$\text{Absolute Error (dB)} = |SNR_N - SNR_E|, \quad (57)$$

To compare the restoration result after filtering, the MSE between two images is defined as

$$MSE = \frac{1}{n_x n_y} \sum_0^{n_x-1} \sum_0^{n_y-1} (r(x, y) - f(x, y))^2, \quad (58)$$

where $r(x, y)$ is reference image and $f(x, y)$ is filtered image. Both images should have the same size $[n_x, n_y]$.

Another common method used to measure the quality of restoration of images is the PSNR, i.e.,

$$PSNR \text{ (dB)} = 10 \log_{10} \left[\frac{\max(r(x, y))^2}{MSE} \right], \quad (59)$$

where $\max(r(x, y))^2$ is the maximum possible pixel value of the reference image.

To measure the similarity between two images, the SSIM formula is used i.e.

$$SSIM(x, y) = \frac{(2\mu_x \mu_y + c_1)(2\sigma_{xy} + c_2)}{(\mu_x^2 + \mu_y^2 + c_1)(\sigma_x^2 + \sigma_y^2 + c_2)}, \quad (60)$$

where μ_x and μ_y are the averages of x and y , σ_x^2 and σ_y^2 are the variances of x and y , σ_{xy} is the covariance between x and y , and c_1 and c_2 are constants that stabilize the computation when the denominators become small.

For the quality index, the equation is defined as

$$Q = \frac{4\sigma_{mn}\bar{p}\bar{q}}{(\sigma_m^2 + \sigma_n^2)[(\bar{x})^2 + (\bar{y})^2]} \quad (61)$$

$$\bar{p} = \frac{1}{N} \sum_{i=1}^N p_i \quad \bar{q} = \frac{1}{N} \sum_{i=1}^N q_i \quad (62)$$

$$\sigma_m^2 = \frac{1}{N-1} \sum_{i=1}^N (p_i - \bar{p})^2 \quad \sigma_n^2 = \frac{1}{N-1} \sum_{i=1}^N (q_i - \bar{q})^2 \quad (63)$$

$$\sigma_{mn} = \frac{1}{N-1} \sum_{i=1}^N (p_i - \bar{p})(q_i - \bar{q}) \quad (64)$$

where N is number of data, $p = \{p_i | i = 1, 2, 3, \dots, N\}$ contains the data of raw image, \bar{p} is the mean of raw image data, $q = \{q_i | i = 1, 2, 3, \dots, N\}$ contains the data of test image and \bar{q} is the mean of test image. The raw and test images must have the same size.

To validate the capability of the NSMAD method in estimating the Rician noise on brain images, different levels of Rician noise are applied. The actual noise standard deviation value, σ_n and the estimated value provided by the NSMAD method, $\hat{\sigma}_E$ is compared. The Standard Error (SE) is used as the error bar to represent the estimation error of noise standard deviation in the measurement. To calculate the error, the SE equation is defined as

$$SE = \frac{\sum_{i=0}^n \left(\frac{\hat{\sigma}_{Ei}}{\sigma_{ni}} - M \right)^2}{n * \sqrt{n}} \quad (65)$$

$$M = \frac{1}{n} \sum_{i=0}^n \frac{\hat{\sigma}_{Ei}}{\sigma_{ni}} \quad (66)$$

where n is the number of data and M is mean of a ratio between actual and estimated standard deviation.

Fig. 4 shows the ratio between $\hat{\sigma}_E$ and σ_n estimated using the NSMAD method on a brain image A.

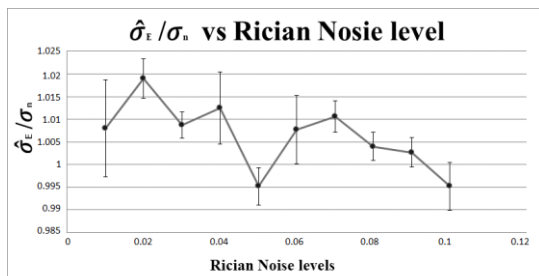


Fig. 4. Ratio between actual and estimated noise standard deviation versus all levels of Rician noise

An error bar is plotted on each point in the line graph to indicate an uncertainty in a value. Based on the overall levels

of Rician noise, the relative error in NSMAD estimation inferior by 2%. Since the acceptance rate of relative error is usually at 5%, this indicates that NSMAD is able to robustly estimate the standard deviation of Rician noise throughout the large range of noise levels.

To validate the reliability of NSMAD on estimating noise standard deviation, a few existing noise estimation methods are compared, as shown in Fig. 5

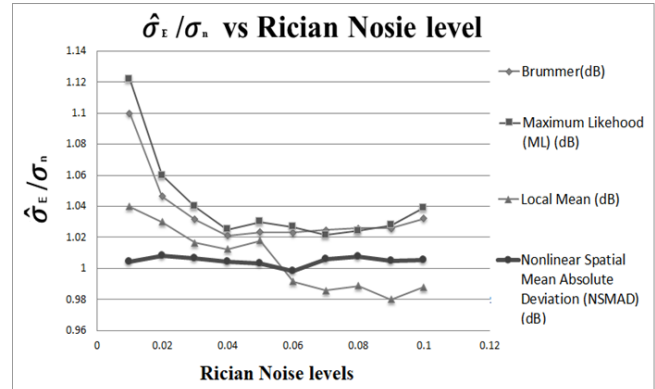


Fig. 5. Result of the existing and NSMAD methods for the entire levels of noise

Fig. 5 shows the ratios between $\hat{\sigma}_E$ and σ_n estimated using Brummer's, ML, Local Mean, and NSMAD methods for all levels of Rician noise. For the ideal case where $\hat{\sigma}_E$ and σ_n equal to each other, the ratio between $\hat{\sigma}_E$ and σ_n is 1. Based on Fig. 5, NSMAD outperforms other noise estimation methods, as the ratio estimated by NSMAD is approximately 1. In addition, the NSMAD performance has less fluctuation throughout all levels of noise as compared with those from other existing methods, indicating its stable estimation on $\hat{\sigma}_E$.

Furthermore, to measure the accuracy of noise estimation methods, the Mean Absolute Error (MAE) metric is used i.e.

$$\text{Absolute Error of } \frac{\hat{\sigma}_{Ei}}{\sigma_{ni}}, E = \left| 1 - \frac{\hat{\sigma}_{Ei}}{\sigma_{ni}} \right| \quad (67)$$

$$MAE = \frac{1}{n} \sum_{i=1}^n E \quad (68)$$

where $\hat{\sigma}_E$ is the estimated noise standard deviation, σ_n is the actual noise standard deviation and n is total noise levels. Fig. 6 shows the MAE scores of NSMAD and existing noise estimation methods.

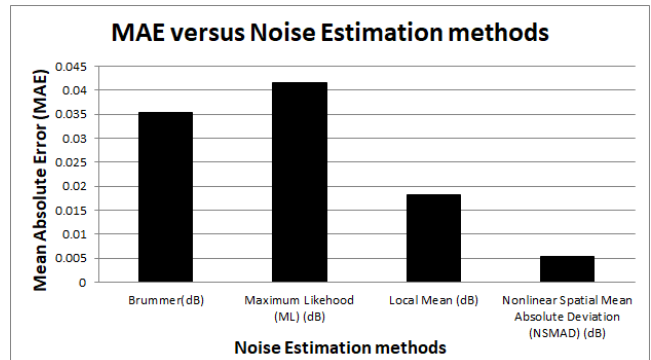


Fig. 6. Mean Absolute Error (MAE) for all noise levels

The MAE equation is used to calculate the mean of the absolute error for all noise levels. A smaller value of MAE indicated a smaller error difference between σ_n and $\hat{\sigma}_E$. Based on Fig. 6, NSMAD yields the smallest MAE value as compared with those from other methods.

To further validate accuracy of noise estimation, the absolute error difference between SNR_N and SNR_E is

computed, which a score approximating zero has the highest accuracy pertaining to estimation of the noise standard deviation. Fig. 7 to 11 show the results of the absolute error, MSE, PSNR, SSIM, and Q of Brummer's, ML, Local Mean, and NSMAD methods with respect to the standard deviation of noise ranging from 0.01 to 0.10, respectively

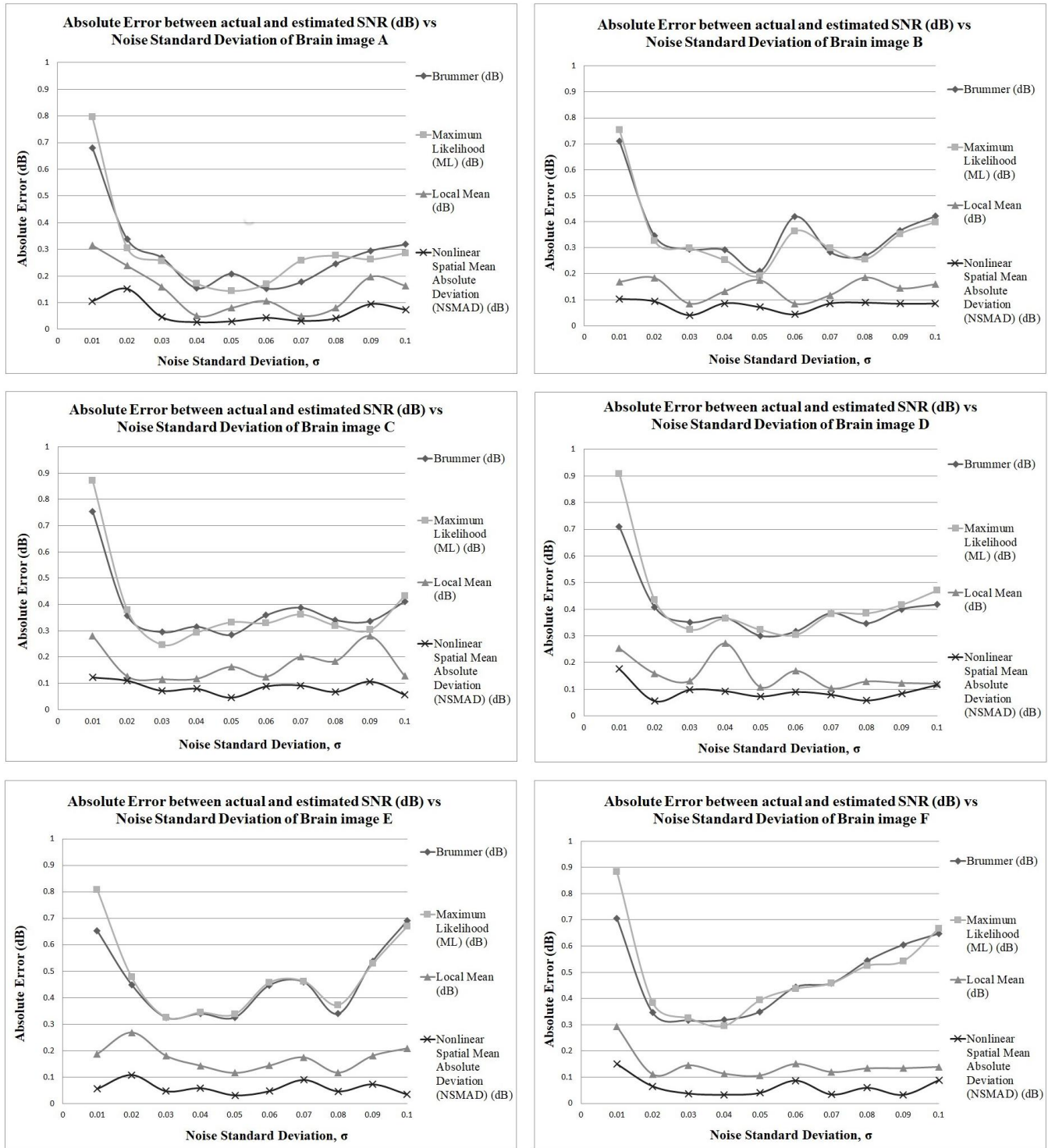


Fig. 7. Absolute Error versus Noise standard deviation of Brain image A, B, C, D, E, and F

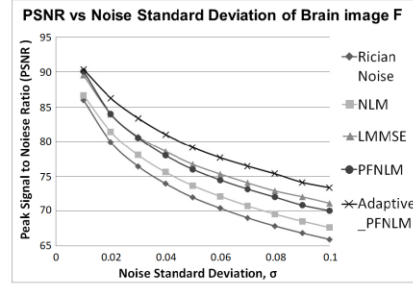
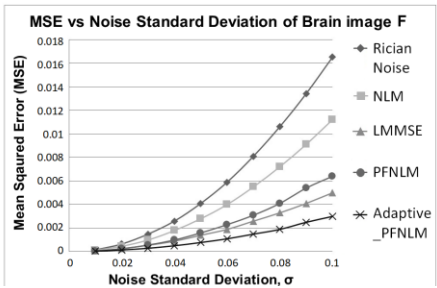
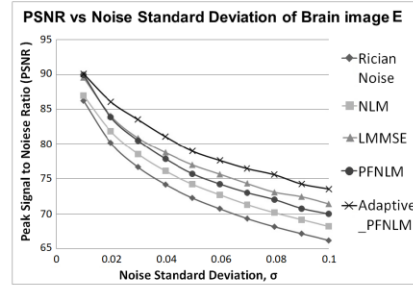
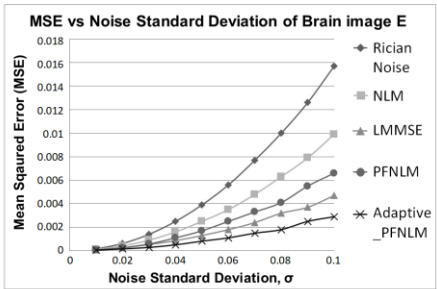
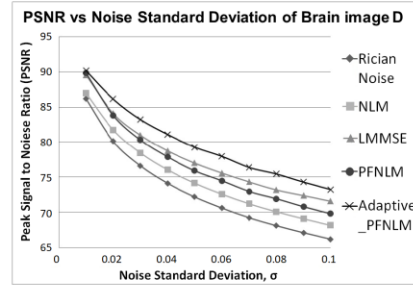
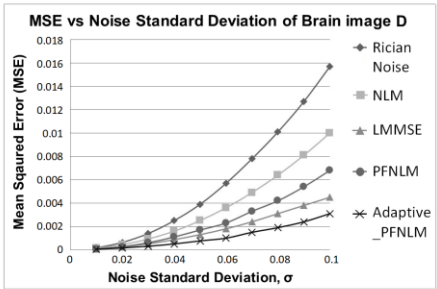
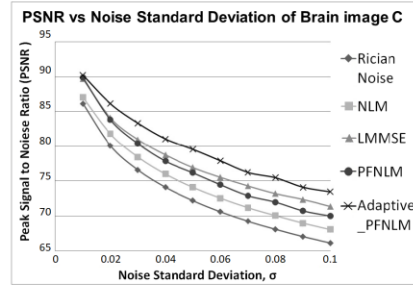
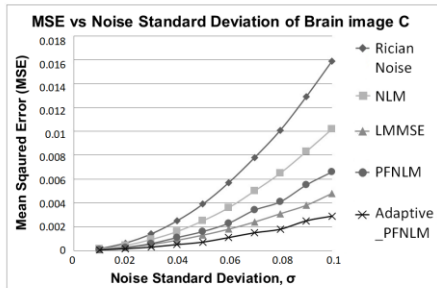
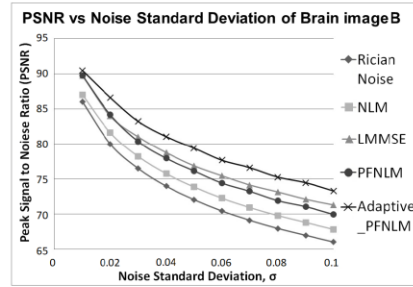
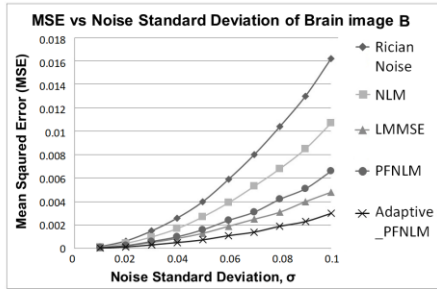
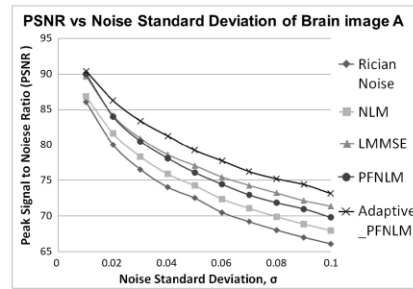
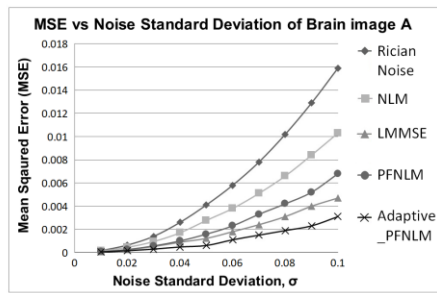


Fig. 8. MSE versus Noise standard deviation of Brain image A, B, C, D, E, and F

Fig. 9. PSNR versus Noise standard deviation of Brain image A, B, C, D, E, and F

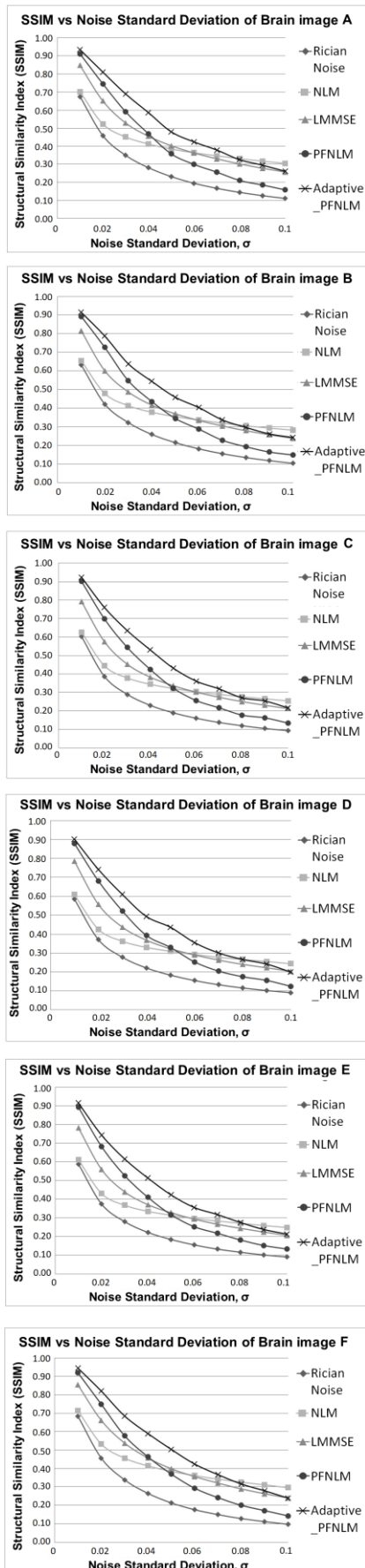


Fig. 10. SSIM versus Noise standard deviation of Brain image A, B, C, D, E, and F

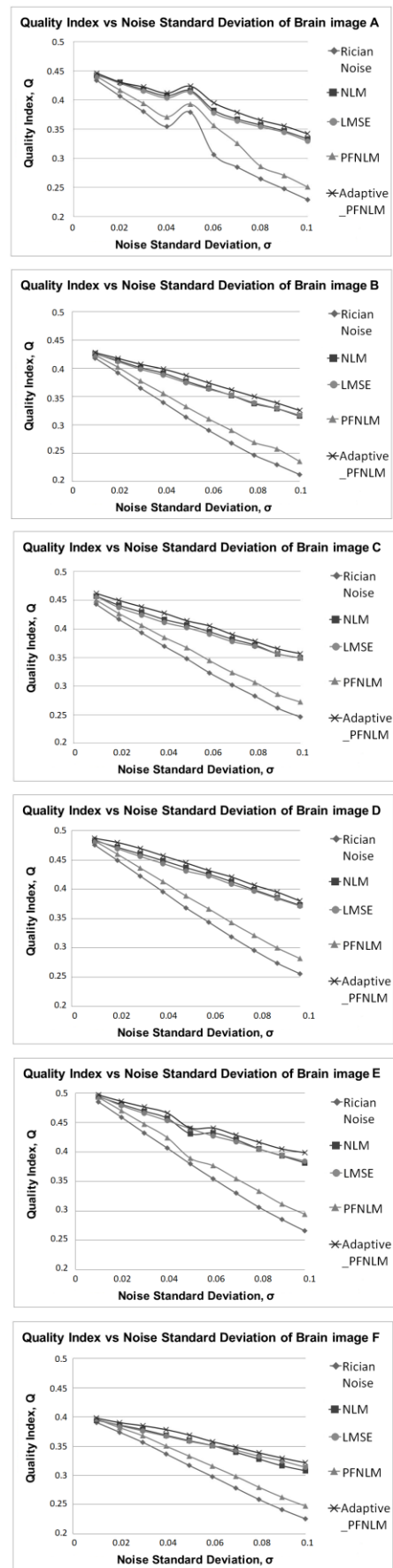


Fig. 11. Quality index versus Noise standard deviation of Brain image A, B, C, D, E, and F

Six MRI images from different levels of slice are used as samples for visual assessment. The images are denoted as A, B, C, D, E, and F respectively. Firstly, all images are corrupted with Rician noise with a variance of 0.10. Then, the

noisy images are filtered by using the NLM, LMMSE, PFNLM, Adaptive_PFNLM filters. The results are shown in Table I.

TABLE I
COMPARISON OF EACH FILTER APPLIED TO BRAIN IMAGES A, B, C, D, E, AND F

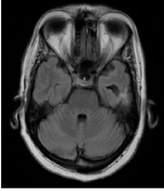
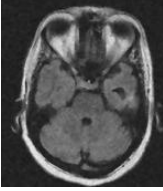
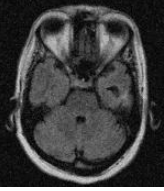
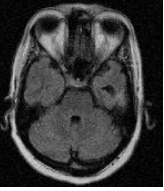
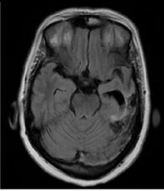
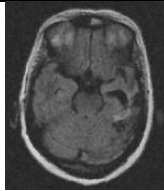
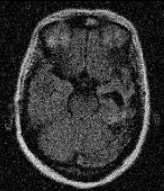
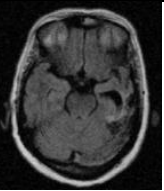
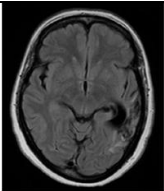
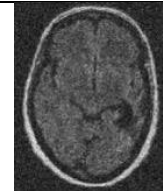
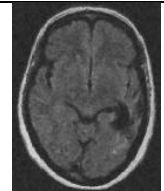
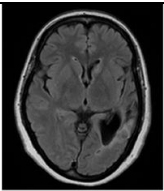
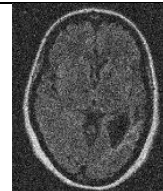
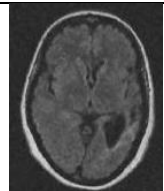
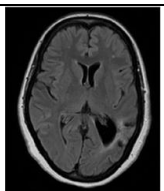
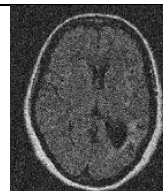
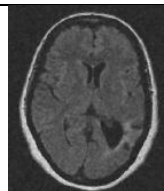
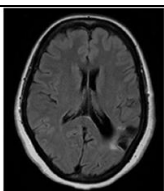
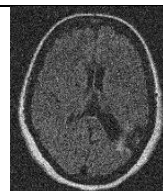
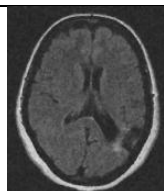
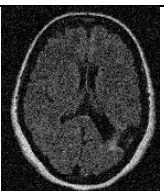
	Original Image	Corrupted Image	NLM Filter	LMMSE Filter	PFNLM Filter	Adaptive PFNLM Filter
A						
B						
C						
D						
E						
F						

TABLE II
ESTIMATE ABSOLUTE ERROR OF $\frac{\hat{\sigma}_E}{\sigma_n}$ AND SNR

Absolute Error of Noise Estimation	$\sigma = 0.01$		$\sigma = 0.05$		$\sigma = 0.10$	
	$\frac{\hat{\sigma}_E}{\sigma_n}$	SNR (dB)	$\frac{\hat{\sigma}_E}{\sigma_n}$	SNR (dB)	$\frac{\hat{\sigma}_E}{\sigma_n}$	SNR (dB)
Brummer's	1.0×10^{-1}	0.6806	2.3×10^{-2}	0.2087	3.2×10^{-2}	0.3186
ML	1.2×10^{-1}	0.7955	3.0×10^{-2}	0.144	3.9×10^{-2}	0.2861
Local Mean	4.0×10^{-2}	0.315	1.8×10^{-2}	0.0806	1.2×10^{-2}	0.1632
NSMAD	4.4×10^{-3}	0.106	3.0×10^{-3}	0.0202	5.3×10^{-3}	0.0739

Table III shows the experimental results of the brain image for two different noise standard deviations, σ . Each column of σ consists of four image quality metrics, namely MSE, PSNR, SSIM and Q.

TABLE III
IMAGE QUALITY METRICS: MSE, PSNR, SSIM, AND QILV FOR THE MRI IMAGE WITH RICIAN NOISE

IMAGE QUALITY METRICS Noise Filter	$\sigma = 0.05$				$\sigma = 0.1$			
	MSE	PSNR	SSIM	Q	MSE	PSNR	SSIM	Q
Rician Noise	3.9×10^{-3}	72.2235	0.3429	0.3797	1.5×10^{-2}	66.1709	0.2163	0.2659
NLM	2.5×10^{-3}	74.1958	0.4371	0.4309	9.9×10^{-3}	68.1674	0.3609	0.3815
LMMSE	1.3×10^{-3}	76.9915	0.4481	0.4396	4.7×10^{-3}	71.3983	0.3587	0.3845
PFNLM	1.7×10^{-3}	75.7162	0.4356	0.3994	6.6×10^{-3}	69.9554	0.2666	0.2942
Adaptive_PFNLM	8.2×10^{-4}	78.967	0.5158	0.4408	2.9×10^{-3}	73.5329	0.3647	0.3988

Table II shows the absolute errors of the experiment. It consists of three different noise standard deviations, σ , each in a separate column. Each column of σ shows the absolute error of $\frac{\hat{\sigma}_E}{\sigma_n}$ and absolute error of SNR (dB).

Based on Fig. 7, both Brummer's and ML methods have the largest absolute errors of SNR, while the Local Mean method produces a moderate absolute error value. The NSMAD method yields the smallest absolute error value as compared with those from the other three methods. For the Local Mean method, it has better SNR estimation than those of the Brummer's and ML methods. However, the accuracy of SNR estimation using the Local Mean method is lower than that of the NSMAD method. Moreover, the absolute error of both Brummer's and ML methods decreases when the standard deviation changes from 0.01 to 0.02. For the standard deviation from 0.02 to 0.10, the trend of both Brummer's and ML methods becomes unstable with fluctuation. In short, both methods begin to estimate poorly when the standard deviation increases. For the Local Mean and NSMAD methods, their performances fluctuate minimally throughout the range of standard deviations. Both methods depict stable estimation on SNR as compared with those of the Brummer's and ML methods.

Referring to Table II, the NSMAD method has the smallest absolute error of $\frac{\hat{\sigma}_E}{\sigma_n}$. This is because the ratio value estimated by NSMAD approximates 1. The NSMAD method also has the smallest absolute error of SNR, as mentioned before. These results ascertain the effectiveness of NSMAD as compared with those of the existing noise estimation methods.

By referring to Figs. 8, 9, 10, and 11, it can be observed that all six filtered MR images share similar image properties. In Figs. 9, 10, and 11, as the noise standard deviation increases from 0.01 to 0.10, the PSNR, SSIM and Q scores decrease gradually. This indicates that when the noise density progressively increases, the quality of MR images progressively decreases. In other words, the noise density is inversely proportional to the quality of images.

Based on the performance of all filters in Table II, Adaptive_PFNLM produces the best overall performance since it is able to efficiently reduce Rician noise in MR images. While PFNLM and Adaptive_PFNLM have similar functionality in removing Rician noise, Adaptive_PFNLM outperforms PFNLM with higher PSNR scores. For the LMMSE filter, its PSNR value is higher than those of PFNLM and NLM filters. But, its performance is still inferior to that of Adaptive_PFNLM. Although the PSNR value of LMMSE is higher than that of PFNLM, its filtered images have slightly low visibility than those of PFNLM filtered images. For the

NLM filter, it produces the lowest PSNR value as compared with those from the other three filters. The NLM filtered images are blurry and have the lowest level of visibility.

Overall, Adaptive_PFNLM yields the highest PSNR performance, which is followed by LMMSE, PFNLM, and lastly NLM. For visibility of filtered images, Adaptive_PFNLM and NLM produce the best and worst quality images, respectively.

V. CONCLUSION

The aim of this research is to design a new noise estimation method to estimate Rician noise and a new noise filter for removing Rician noise from MR images. Based on the empirical absolute error results, the proposed NSMAD method is able to achieve the highest accuracy rates pertaining to estimation of various noise levels as compared with those of three existing methods.

The noise-removing technique is based on cascading the NSMAD method with an Adaptive_PFNLM filter. The proposed Adaptive_PFNLM filter is developed by concatenation of PFNLM and a 2-D Adaptive Noise-Removal filter. Adaptive_PFNLM achieves the best MSE, PSNR, SSIM, and Q results as compared with those of three existing methods, namely NLM, LMMSE, and PFNLM filters. Furthermore, the proposed filter produces better quality of visibility in MR images as compared with those from the NLM filter.

ACKNOWLEDGEMENT

The authors gratefully thank Telekom Research & Development Sdn Bhd (TM R&D) for supporting this research. This paper is based on the research supported by TM R&D grant (RDTC/180974).

REFERENCES

- [1] F. F. Ting, K. S. Sim, and E. K. Wong, "A rapid medical image noise variance estimation method," in *2016 International Conference on Robotics, Automation and Sciences (ICORAS)*, 2016, pp. 1–6.
- [2] S. Shen, W. Sandham, M. Granat, and A. Sterr, "MRI fuzzy segmentation of brain tissue using neighbourhood attraction with neural-network optimization," *IEEE Trans. Inf. Technol. Biomed.*, vol. 9, no. 3, pp. 459–467, 2005.
- [3] I. Aarya, D. Jiang, and T. Gale, "Edge localisation in MRI for images with signal-dependent noise," *Electron. Lett.*, vol. 51, no. 15, pp. 1151–1153, 2015.
- [4] R. D. Nowak, "Wavelet-based Rician noise removal for magnetic resonance imaging," *IEEE Trans. Image Process.*, vol. 8, no. 10, pp. 1408–1419, 1999.
- [5] J. Hari Haran, G. Ajith Bosco Raj, T. "Efficient denoising of rician noisy magnetic resonance brain images using self," *Int. J. Adv. Eng. Technol.*, vol. 7, no. 2, pp. 638–642, 2016.
- [6] V. V.R., P. T. Vanathi, and P. Kanagasabapathy, "Fast and efficient algorithm to remove gaussian noise in digital images," *IAENG Int.*

- [7] *J. Comput. Sci.*, vol. 37, pp. 78–84, 2010.
- [8] S. Aja-Fernández, C. Alberola-López, and C. F. Westin, "Noise and signal estimation in magnitude MRI and Rician distributed images: A LMMSE approach," *IEEE Trans. Image Process.*, vol. 17, no. 8, pp. 1383–1398, 2008.
- [9] J. Sijbers, "Signal and noise estimation from magnetic resonance images," *Diss. Abstr. Int.*, vol. 59–9, no. B, p. 4892, 1998.
- [10] H. Gudbjartsson and S. Patz, "The Rician distribution of noisy MRI data," *Magn. Reson. Med.*, vol. 34, no. 6, pp. 910–914, Dec. 1995.
- [11] L. Cadena, A. Zotin, F. Cadena, A. Korneeva, and A. Legalov, "Noise reduction techniques for processing of medical images," *Proc. World Congr. Eng. 2017*, vol. I, pp. 496–500, 2017.
- [12] J. Sijbers, D. Poot, A. J. den Dekker, and W. Pintjens, "Automatic estimation of the noise variance from the histogram of a magnetic resonance image," *Phys. Med. Biol.*, vol. 52, no. 5, pp. 1335–48, 2007.
- [13] J. Rajan, "Estimation and removal of noise from single and multiple coil magnetic resonance images Schatting en verwijdering van ruis in magnetische-resonantiebeelden opgemeten met één of meerdere spoelen Supervisor :," no. November, 2012.
- [14] M. G. Péreza, A. Conci, A. B. Morenoc, V. H. Andaluza, and J. A. Hernández, "Estimating the Rician noise level in brain MR image," pp. 2–7.
- [15] R. D. Nowak, D. J. Nowak, R. G. Baraniuk, and R. S. Hellman, "Wavelet domain filtering for nuclear medicine imaging," in *1996 IEEE Nuclear Science Symposium. Conference Record*, 1996, vol. 3, pp. 1802–1806 vol.3.
- [16] A. Buades, B. Coll, and J.-M. J.-M. Morel, "A non-local algorithm for image denoising," *Comput. Vis. Pattern Recognition, 2005. CVPR 2005. IEEE Comput. Soc. Conf.*, vol. 2, no. 0, pp. 60–65, 2005.
- [17] A. Tristán-Vega, V. García-Pérez, S. Aja-Fernández, and C. F. Westin, "Efficient and robust nonlocal means denoising of MR data based on salient features matching," *Comput. Methods Programs Biomed.*, vol. 105, no. 2, pp. 131–144, 2012.
- [18] R. C. Gonzalez and R. E. Woods, *Digital image processing*. Prentice Hall, 2002.
- [19] A. S. Y. Bin-habtoor and S. S. Al-amri, "Removal speckle noise from medical image using image processing techniques," *Int. J. Comput. Sci. Inf. Technol.*, vol. 7, no. 1, pp. 375–377, 2016.
- [20] A. Martin, J. F. Garamendi, and E. Schiavi, "Mr-Dti Rician Denoising," *Dyna*, Vol. 80, Pp. 25–30, 2013.
- [21] D. M. Drumheller, "General expressions for Rician density and distribution functions," *IEEE Trans. Aerosp. Electron. Syst.*, vol. 29, no. 2, pp. 580–588, 1993.
- [22] M. K. Simon, *Probability distributions involving gaussian random variables*, vol. 683, no. 0, 2002.
- [23] M. E. Brummer, R. M. Mersereau, R. L. Eisner, and R. R. J. Lewine, "Automatic detection of brain contours in MRI data sets," *IEEE Trans. Med. Imaging*, vol. 12, no. 2, pp. 153–166, 1993.
- [24] P. Garhwal and P. Garhwal, "Image denoising with linear and non-linear filters : A," *IJCSI Int. J. Comput. Sci. Issues*, vol. 10, no. 6, pp. 149–154, 2013.
- [25] J. C. Russ, "Image enhancement in spatial domain," *Image Process. Handb.*, vol. 1, no. pag 110, pp. 269–297, 2011.
- [26] K. S. Sim and C. K. Toa, "Nonlinear spatial domain first order moment estimation in magnitude resonance imaging data," in *2016 International Conference on Robotics, Automation and Sciences (ICORAS)*, 2016, pp. 1–5.
- [27] T. Pham-Gia and T. L. Hung, "The mean and median absolute deviations," *Math. Comput. Model.*, vol. 34, no. 7, pp. 921–936, 2001.
- [28] T. Pieciak, S. Aja-Fernandez, and G. Vegas Sanchez-Ferrero, "Non-Stationary Rician noise estimation in parallel MRI using a single image: a Variance-Stabilizing Approach," *IEEE Trans. Pattern Anal. Mach. Intell.*, vol. XX, no. c, pp. 1–1, 2016.